ELSEVIER

Arthropod Structure & Development 29 (2000) 343–353

ARTHROPOD STRUCTURE & DEVELOPMENT

www.elsevier.com/locate/asd

Structural organization of the sex pheromone gland in *Helicoverpa zea* in relation to pheromone production and release☆

Ashok K. Raina[a,*], William P. Wergin[b], Charles A. Murphy[b], Eric F. Erbe[b]

[a]*Formosan Subterranean Termite Research Unit, USDA, ARS, 1100 Robert E. Blvd., New Orleans, LA 70179, USA*
[b]*Nematology Laboratory, USDA, ARS, Bldg. 477A, Beltsville, MD 20705, USA*

Received 28 November 2000; accepted 1 March 2001

Abstract

Morphological location of the sex pheromone producing area in the ovipositor of the female corn earworm *Helicoverpa zea*, was correlated with gas chromatographic analysis of the extracted pheromone. Histological studies showed that the pheromone gland occupied an almost complete ring of specialized columnar cells between the 8th and 9th abdominal segments. Ultrastructure of the pheromone gland cells revealed distinct features such as microvilli, pockets of granular material, intercellular canals with abundant desmosomes. Apparent changes in some of these features are associated with phases of pheromone production and non-production. Examination of the tissue with low temperature scanning electron microscopy showed the presence of excreted droplets at the tips of cuticular hairs in the glandular area during the period of pheromone production. Published by Elsevier Science Ltd.

Keywords: Sex pheromone gland; Morphology; Low temperature SEM; Ultrastructure

1. Introduction

Females of most moths produce species-specific sex pheromones in specialized glands, generally located on the terminal abdominal segments that constitute the ovipositor. Percy-Cunningham and MacDonald (1987) identified the pheromone glands of female moths representing 16 families and studied their structural characteristics. The majority of the species examined belong to the family Noctuidae. Among the Heliothinae, morphology and histology of the pheromone glands were studied in *Heliothis virescens* and *Helicoverpa zea* (Jefferson et al., 1968; Aubrey et al., 1983; Teal et al., 1983; Percy-Cunningham and MacDonald 1987). Percy-Cunningham and MacDonald (1987) reported on ultrastructural features of the gland in *H. zea*. A more complete ultrastructural study of the pheromone glands was conducted in *Choristoneura fumiferana* (Percy, 1974) and *Trichoplusia ni* (Percy, 1979). In the latter case, the author also attempted to correlate ultrastructural changes to production and release of pheromone. In spite of all these studies questions remain unanswered. Although, the general position of the pheromone gland is described no definitive information exists about the extent of the glandular area. Additionally, no attempts have correlated actual pheromone titers with structural changes and very little is known about areas associated with pheromone release.

Sex pheromone in *H. zea* is a blend of four components, with (*Z*)-11-hexadecenal comprising over 90% (Klun et al., 1979). Raina et al., 1986 demonstrated the diel periodicity of pheromone production in *H. zea* and the involvement of a neuropeptide hormone in the regulation of pheromone production in this and other species of moths (Raina et al., 1989). These studies indicated that pheromone production could be experimentally manipulated in *H. zea* females, and thus correlated with ultrastructural changes in the gland during pheromone production. In the present study, pheromone titer in various sections of the ovipositor were determined with greater precision by gas chromatographic analysis and compared to histological preparations. In addition, transmission electron microscopy and low temperature scanning electron microscopy were used to observe morphological features and to determine if structural changes could be correlated to pheromone production and release.

☆ Mention of a product does not constitute an endorsement by the US Department of Agriculture.

* Corresponding author. Tel.: +1-504-286-4290; fax: +1-504-286-4235.
E-mail address: araina@nola.srrc.usda.gov (A.K. Raina).

1467-8039/01/$ - see front matter. Published by Elsevier Science Ltd.
PII: S1467-8039(01)00014-7

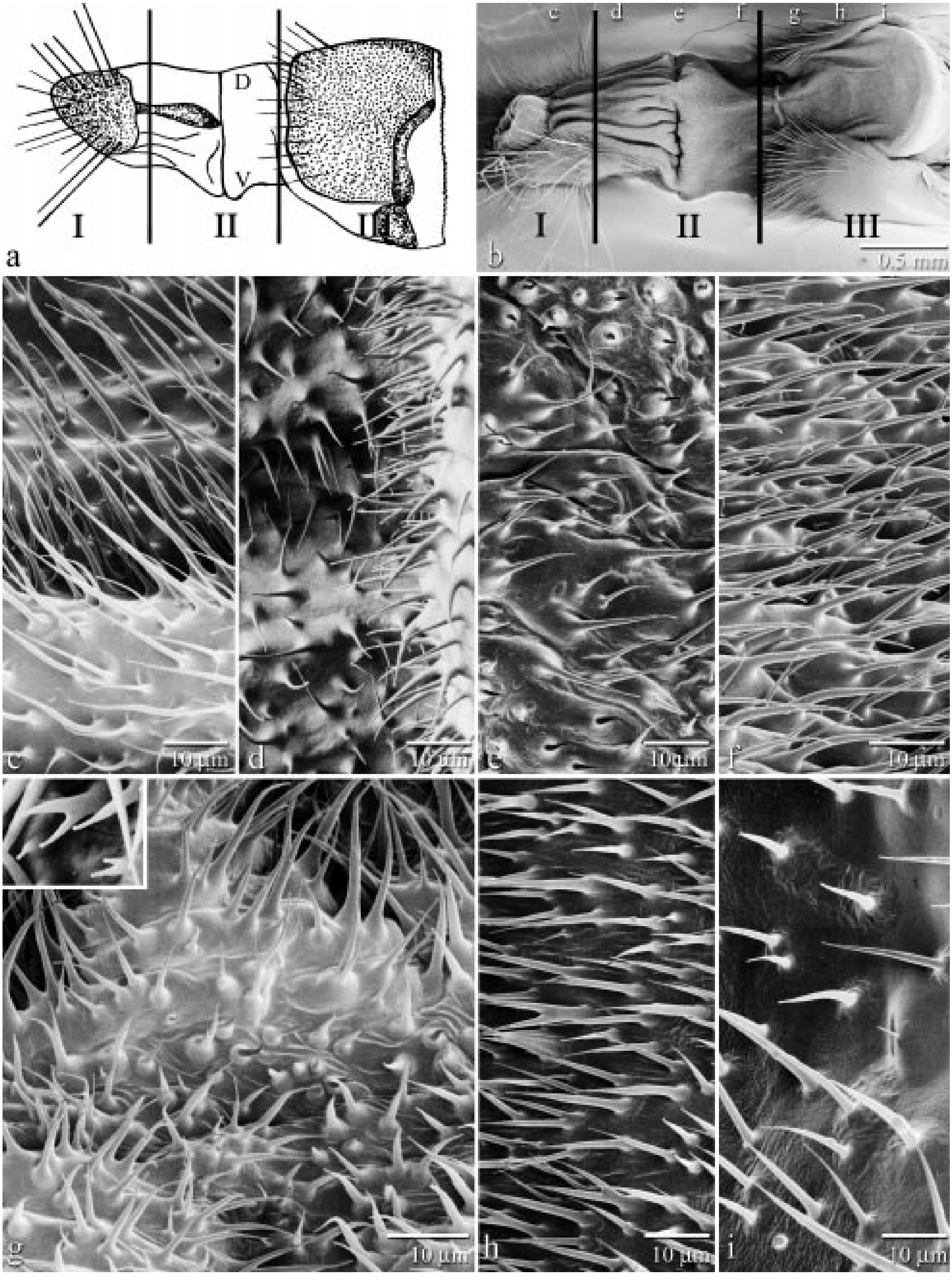

D
V
I
II
III
a
c
d
e
f
g
h
i
b
0.5 mm
10 µm

2. Materials and methods

2.1. Insect rearing

H. zea eggs were obtained from a laboratory culture at Stoneville, MS. The resulting larvae were reared on artificial diet, and maintained in environmental chambers at 16 L (26°C): 8 D (22°C) and 60–65% RH. Male and female pupae were placed in separate chambers for adult emergence. Adults were provided 10% sucrose solution for feeding.

2.2. Pheromone determinations

Intact females taken during second photophase and neck-ligated females were used as the source of pheromone-less glands. Intact females taken during third scotophase or ligated females injected with 5 pmol pheromone biosynthesis activating neuropeptide (PBAN) 2–3 h before excising the ovipositor, provided glands with pheromone. Ovipositors (8th and 9th abdominal segments) were excised from the above females and extracted in heptane containing an internal standard. The extracts were analyzed by gas chromatography (Raina et al., 1986). Five ovipositors from scotophase females were each cut into three parts as shown in Fig. 1(a). Each part was individually extracted and analyzed for pheromone. Finally the middle part was further sliced into dorsal and ventral portions and each portion analyzed for pheromone.

2.3. Histology

Retracted and fully extended (by applying slight pressure on the abdomen) ovipositors from females in both photophase and scotophase were fixed in aqueous Bouin's fixative. After dehydration, the specimens were embedded in wax and serial sectioned. Sagittal and cross sections, 6 μm thick, were stained with Mallory's triple stain and examined with an Olympus BX60 microscope.

2.4. Low temperature scanning electron microscopy

Ovipositors of photophase and scotophase females were excised and attached to a copper specimen holder with a cryo-adhesive (Tissue Tek, Ted Pella Inc., Redding, CA). The holders were plunged into liquid nitrogen and then cryo-transferred under vacuum to a cold stage in the pre-chamber of an Oxford CT-1500 HF Cryosystem. The frozen specimens were etched for about 10 min in the pre-chamber by raising the temperature of the stage to −90°C. Next the temperature was lowered and the samples were sputter coated with platinum and then transferred to the cryo-stage in a S-4100 field emission SEM (Hitachi Scientific Instuments, Mountain View, CA) for observation. Accelerating voltages of 10–15 kV were used to view the specimens.

2.5. Transmission electron microscopy

Small sections (1–2 mm^2) were cut from the pheromone gland area, located on the ventral side of the ovipositor and prepared for electron microscopy as previously described (Wergin and Endo, 1976). Briefly, dissected tissue was placed in buffered 3% glutaraldehyde (0.05 M phosphate buffer, pH 6.8) at 22°C for 2 h. Following primary chemical fixation, the samples were washed for 1 h in six changes of the buffer, post-fixed in buffered 2% osmium tetroxide for 2 h, rinsed in buffer, dehydrated in an acetone series, and infiltrated with Spurr's low viscosity embedding medium (Spurr, 1969). In an attempt to optimize the chemical fixation and resin infiltration two variations of this procedure were also used. First, microwave irradiation was performed in a domestic Amana Microwave Oven (Amana Refrigeration, Inc., Amana, IO) at 500 W. A beaker containing 400 ml of distilled water was placed in the rear of the oven to act as the heat sink. Vials containing dissected tissue in the 3% buffered glutaraldehyde were irradiated continuously at a 'high' setting for 30 s and then transferred to fresh fixative at room temperature. All subsequent washing, post-fixation, dehydration and infiltration was done as described above. Secondly, tissues were fixed in a mixture of 3% glutaraldehyde, 1.5% formaldehyde and 1.5% acrolein in 0.1 M sodium cacodylate buffer (EM Sciences, Ft. Washington, PA). Following fixation, the samples were washed in two changes of the cacodylate buffer, post-fixed for 1 h in 1% Sorenson's phosphate buffered osmium tetroxide, washed in buffer, dehydrated in an alcohol series and infiltrated in Spurr's medium as described above.

Silver-grey sections of selected areas of the tissue were cut on a Reichert/AO Ultracut (Leica, Deerfield,

Table 1
Pheromone content in various sections of the ovipositor of *H. zea*. Female as shown in Fig. 1(a).

Ovipositor section	Pheromone (ng) average ± SD ($N = 5$)
I	7.6 ± 2.8
II	40.7 ± 13.4
III	9.9 ± 2.6
II D (dorsal)	21.7 ± 7.6
II V (ventral)	24.2 ± 5.9

Fig. 1. (a) Schematic drawing of lateral view of the extended ovipositor of *Helicoverpa zea* female showing the three sections (I, II and III) and dorsal (D) and ventral (V) regions of section II, extracted for pheromone, stippled areas indicate heavily sclerotized cuticle; (b) SEM micrograph of ventral surface of the ovipositor (8th and 9th abdominal segments) showing the three sections corresponding to those in a; (c–i) Various regions (marked in b) showing size, density and orientation of cuticular hairs. Inset in g shows bifurcated hairs.

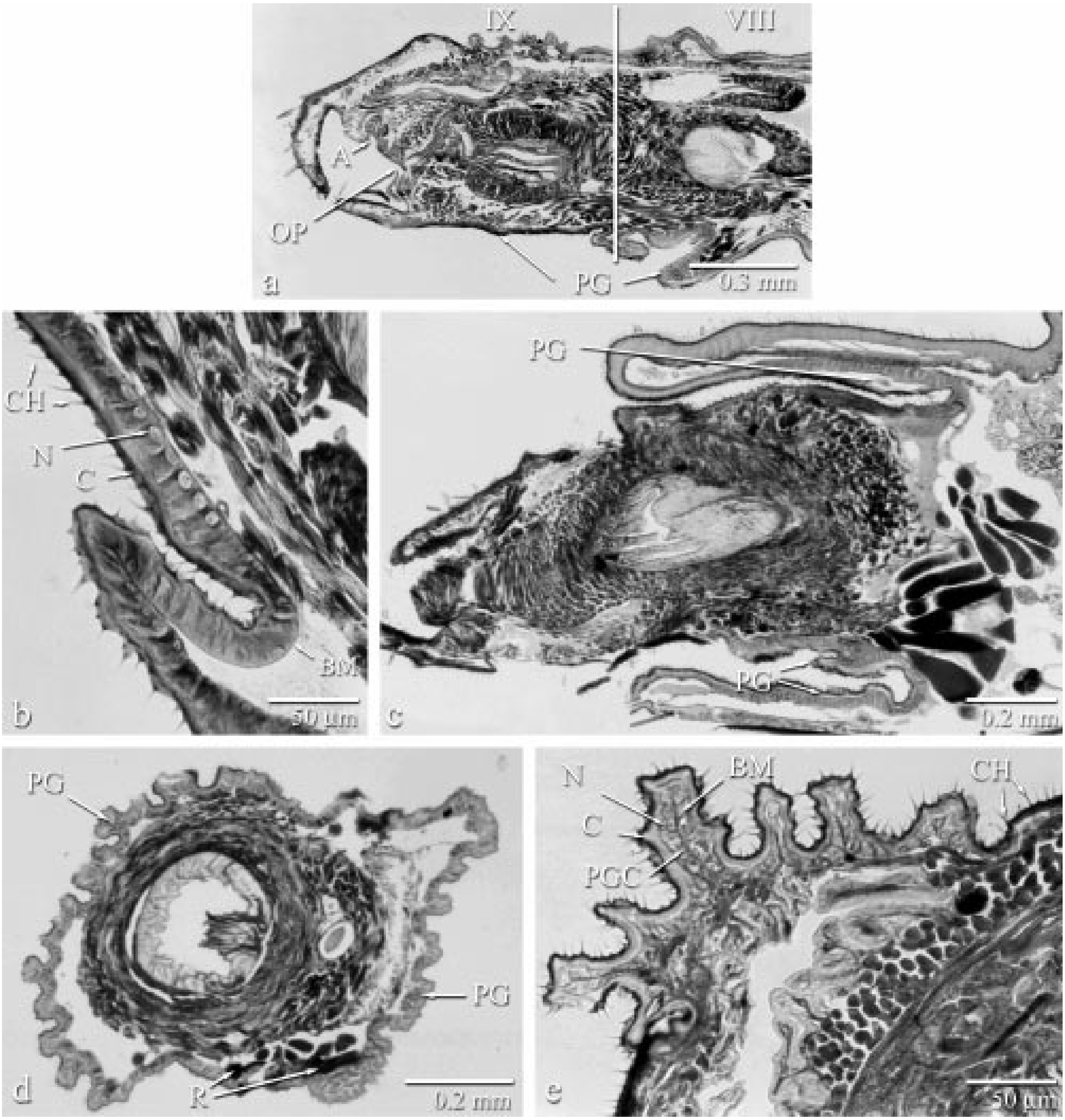

Fig. 2. Light micrographs of ovipositor and pheromone gland: (a) Longitudinal section of fully extended 8th and 9th segments showing pheromone gland (PG) cells in both dorsal and ventral areas (vertical line indicates the segmental divide); (b) large columnar cells in ventral part of the gland; (c) longitudinal section through retracted ovipositor; (d) cross section through 9th segment showing an almost continuos ring of glandular cells; (e) PG cells in the convoluted portion of the 9th segment. A = anus; BM = basement membrane; C = cuticle; CH = cuticular hair; N = nucleus; OP = ovipore; PGC = pheromone gland cell; R = retractor muscle.

Fig. 3. TEM micrographs showing details of PG cells: (a) Columnar gland cells of a photophase female showing large nuclei (N) and a compact layer of microvilli (MV); (b) cells in photophase show large number of small vesicles; (c) columnar gland cells of a scotophase female showing large basal nuclei, pockets of granular material (GM), microtubules (Mt) and desmosomes (D). T = tracheoles.

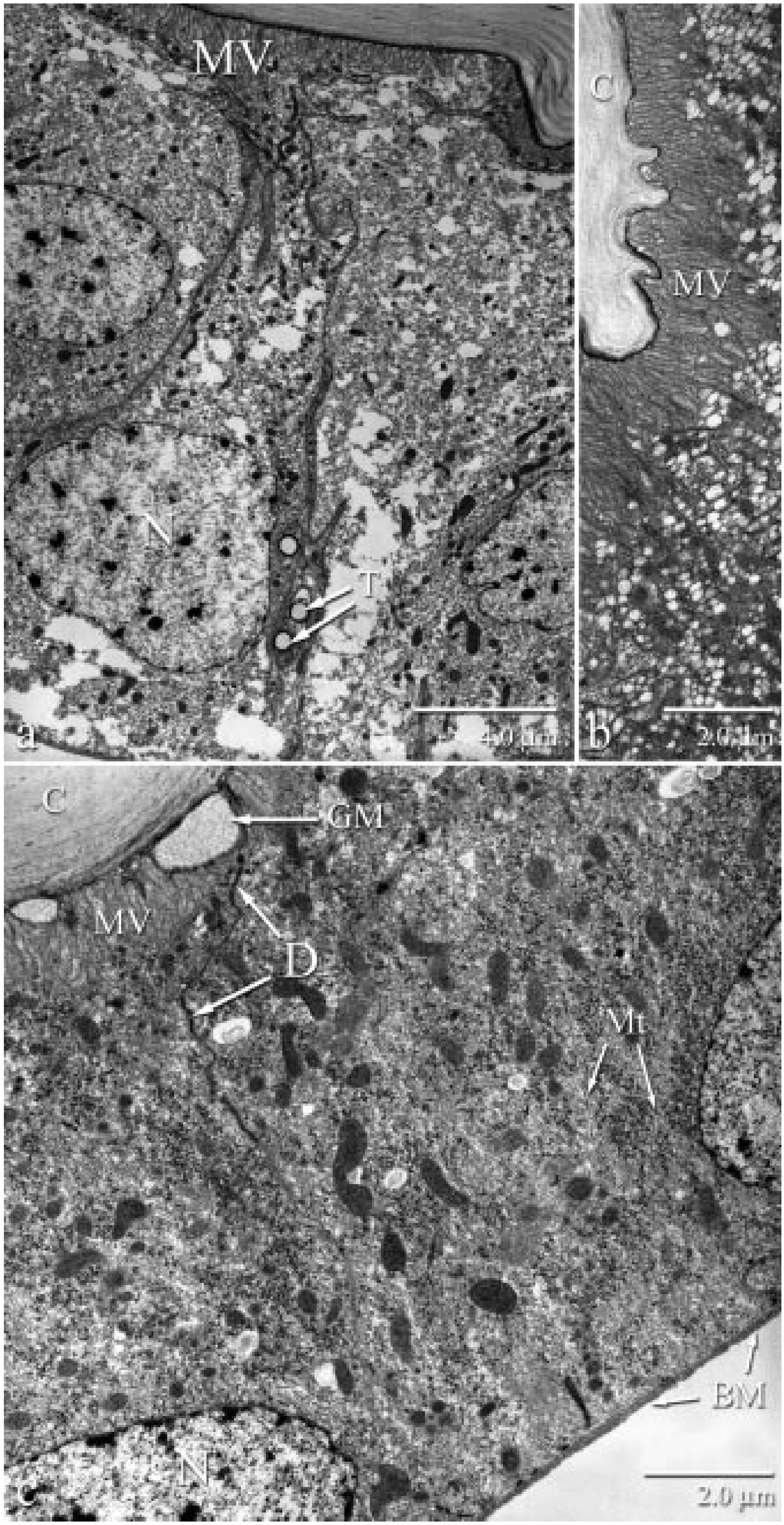
MV
N
T
a
4.0 μm
C
MV
b
2.0 μm
C
GM
MV
D
Mt
BM
N
c
2.0 μm

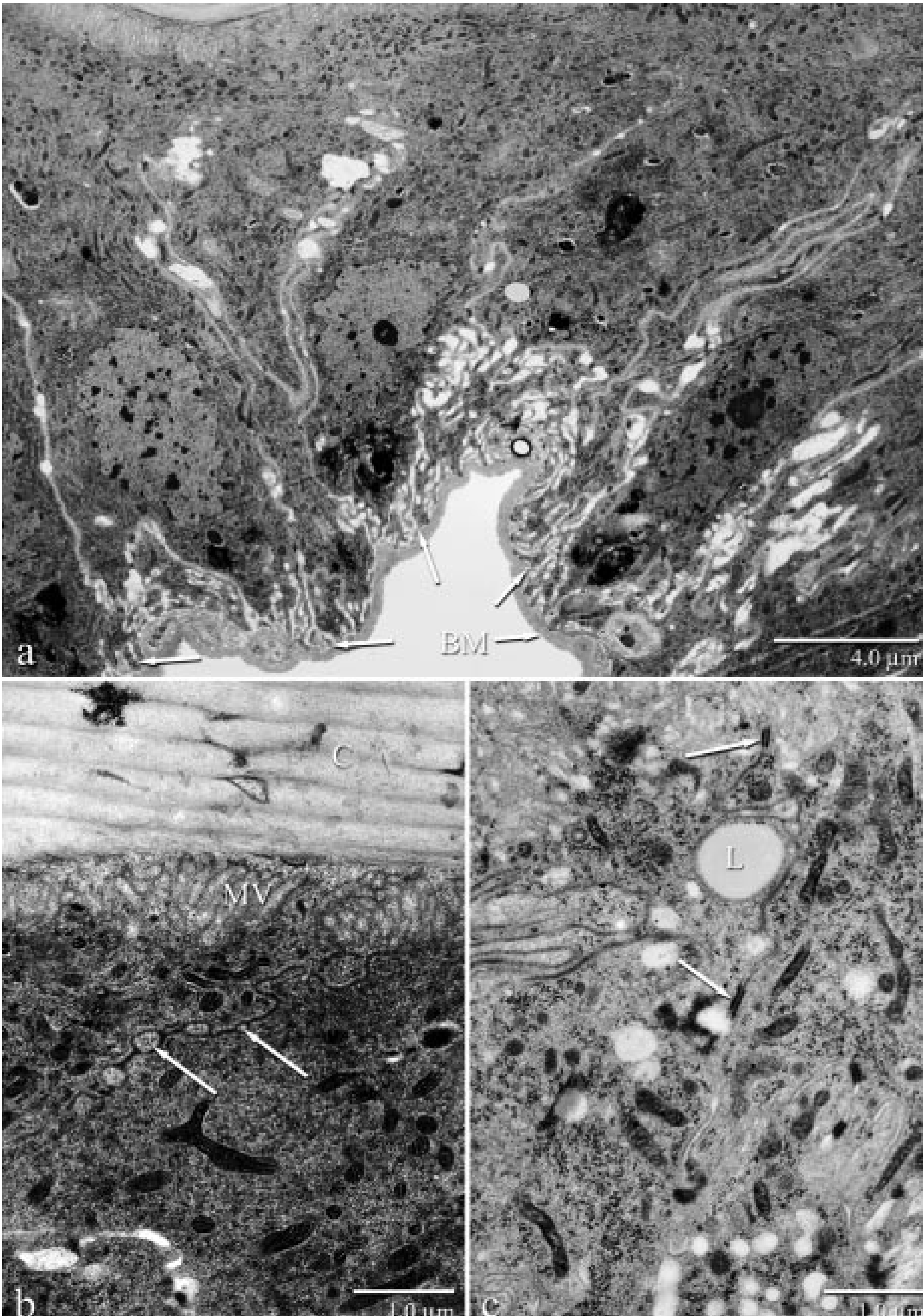
a
BM
4.0 μm
C
MV
b
1.0 μm
L
c
1.0 μm

IL) microtome with a Diatome (Diatome US, Fort Washington, PA) diamond knife and mounted on 400 mesh grids. The sections were stained with 2.5% uranyl acetate in a 50/50 ethanol/water solution for 1 h, then with 3% lead citrate for 5 min. Thin sections were viewed in either a Hitachi H-500 or a Hitachi H-7000 transmission electron microscope operating at 75 kV with a 30 μm objective aperture. Images were recorded on Kodak film using a 2 s exposure. A total of 26 tissue samples representing pheromone producers and non-producers were examined.

3. Results

3.1. Pheromone gland location and morphology

Gas chromatographic analysis of extracts of the ovipositor (8th and 9th abdominal segments) of two day old *H. zea* females during scotophase indicated the presence of >100 ng of pheromone. During the corresponding photophase, the titer was generally <1 ng. Dividing the ovipositor into three regions (Fig. 1(a)), and analyzing extracts from each, indicated that an average of 69.9% of the total pheromone was present in the middle section (Table 1). Regions I and III had 13.0 and 17.1% pheromone, respectively. When region II was divided into dorsal and ventral parts and pheromone titer in each part determined, the dorsal part had an average of 47.2% and the ventral 52.8%. Based on these results, the pheromone gland in *H. zea* is present between the 8th and 9th abdominal segments and occupies both dorsal and ventral regions.

Low temperature SEM of the 8th and 9th segments showed that the latter segment, in particular the ventral surface, was highly convoluted (Fig. 1(b)). The ventral median region of the 9th segment had cuticular hairs which were as long as 16 μm and pointed posteriorly (Fig. 1(c)). The hairs gradually shortened towards the inter-segmental area, and were laterally directed along the ridges (Fig. 1(d)). At the ridge, marking the junction of the two segments, the hairs were very short and pointed in different directions (Fig. 1(e)). Anterior to this region, the hairs lengthened but pointed anteriorly (Fig. 1(f)). In the mid-ventral region of the 8th segment, several smaller ridges formed a star shape. The hairs in this region varied in length, pointed in different directions and some had a bifurcated structure (Fig. 1(g)). From this region to the junction between the 8th and 7th segments, the hairs gradually became shorter and more sparse; all of them pointed posteriorly (Fig. 1(h,i)).

3.2. Histology

Sagittal sections of a retracted ovipositor indicated two folds: the 9th segment was almost completely covered by the 8th segment and the two telescoped segments were covered dorsally by the 7th segment (Fig. 2(c)). In an extended ovipositor, the 8th and 9th segments became fully exposed (Fig. 2(a)). The putative pheromone gland cells appeared as an almost continuous ring having two short breaks in the mid-lateral region (Fig. 2(d)). These cells were most prominent around the base of the fold between the 8th and the 9th segments, and this area had no direct exposure to the outside while the ovipositor was retracted. Extensive convolutions of the dorsal and ventral surfaces were evident in cross sections of the 9th segment (Fig. 2(e)). Pheromone gland cells consisted of a single layer of two types of cells; one type comprised of large columnar cells, about 25–30 μm long and 12–15 μm wide, had prominent spherical nuclei located at their bases (Fig. 2(b)). Some of these cells in scotophase females contained electron opaque spherical bodies. Cells of the second type, which were present in the depressions of the folds, were narrower and had smaller lobed nuclei (Fig. 2(e)). The cuticle was covered with cuticular hairs or spines, with the longer hairs facing in the same direction when the ovipositor was fully retracted.

3.3. Ultrastructure

The larger cells in the ventral part of the pheromone gland had large round nuclei located in the basal region (Fig. 3(a)). The cells had a characteristic layer of microvilli just beneath the endocuticle. The endocuticle and the epicuticle had 12–13 and 7–8 lamellae, respectively. The epicuticle was more dense than the endocuticle. During photophase, cells of the pheromone gland became highly vesiculated with smaller vesicles accumulated just below the microvilli (Fig. 3(b)). A thin layer of electron opaque material accumulated at the tips of the microvilli next to the endocuticle. No obvious Golgi bodies were observed in these cells. During scotophase, pockets of granular material appeared throughout the cell region including within the microvilli (Fig. 3(c)). The cytoplasm was very rich in rough endoplasmic reticulum and mitochondria. In addition, intercellular canals with distinct desmosomes were of common occurrence. No electron opaque band between the microvilli and the endocuticle was present in scotophase cells.

The narrow cells of the gland also had prominent nuclei (Fig. 4(a)). Basal portions of these cells showed invaginations that appeared to arise from the basement membrane

Fig. 4. (a) Columnar cells in the convoluted area of PG in a photophase female showing irregular shaped nuclei and large number of inter- and intracellular canals (arrows), a large number of autophagic bodies (lysosomes) are also seen; (b) some of these canals have a beaded appearance (arrows); (c) during scotophase these cells have numerous desmosomes (arrows) and rough endoplasmic reticulum. BM = basement membrane; C = cuticle; L = lipid sphere.

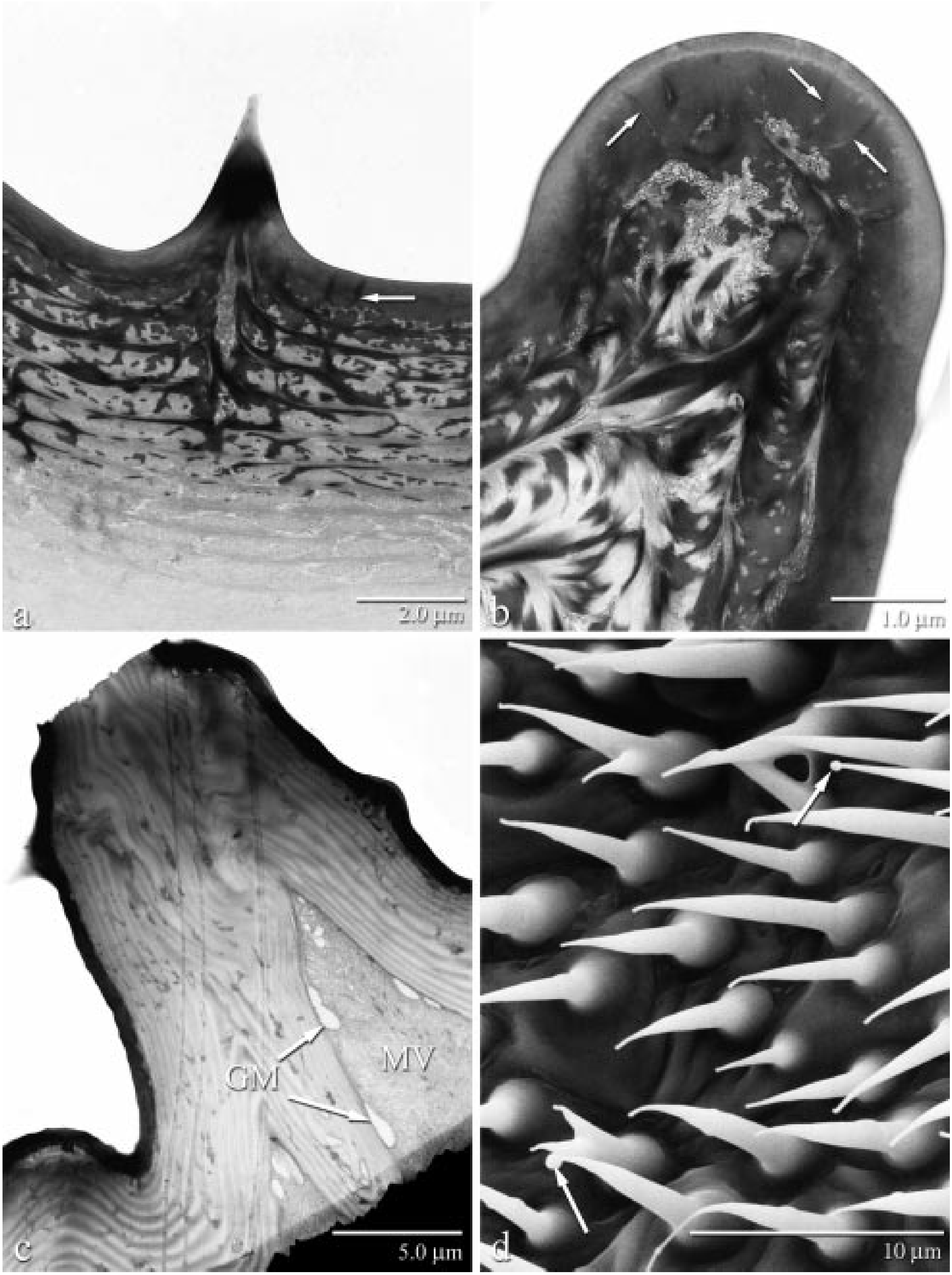
a
2.0 μm
b
1.0 μm
GM
MV
c
5.0 μm
d
10 μm

and continued as inter- and intracellular canals towards the apex of the cell. Some of these canals contained electron opaque granules that appeared to accumulate towards the apex of the cell (Fig. 4(b)). The cytoplasm of these cells had numerous mitochondria and free ribosomes and a few lipid droplets besides a number of autophagic bodies or lysosomes. Apically the cells exhibited the layer of microvilli, similar to that in the larger cells. In scotophase, numerous desmosomes associated with the intracellular canals became prominent (Fig. 4(c)).

The cuticular hairs, which were extensions of the epicuticle, had a hollow core and many pore canals (Fig. 5(a,b)). Short-filamentous material also appeared in the central cavity of the cuticular hairs and in the pore canals (Fig. 5(b)). In narrow folds of the cuticle, the cytoplasm, particularly the apical microvilli, was found in the cavity formed by the endocuticle (Fig. 5(c)).

3.4. Pheromone release

Low temperature SEM revealed the presence of small globules of secretion, at the bases and at the tips of many of the cuticular hairs (Fig. 5(d)). These secretions were observed only in the ventral intersegmental area between the 8th and the 9th segments, and only during scotophase.

4. Discussion

Gas chromatographic determination of pheromone content in various sections of the ovipositor of *H. zea* females revealed that the bulk of the pheromone producing area occupied the adjoining sections of the 8th and 9th segments. Histology of this area showed a single layer of columnar cells that formed an almost continuous ring just below the cuticle. Both dorsal and ventral surfaces in this area had extensive convolutions that were more prominent in the 9th segment. At the ultrastructural level the pheromone gland cells showed characteristic apical microvilli. In females that were producing pheromone, these cells contained pockets of granular material and inter- and intracellular canals with distinct desmosomes. The cuticular hairs had a hollow core and many pore canals. We speculate that pheromone or its immediate precursor, produced in the glandular cells, is transported through the cuticle on to the cuticular hairs. During calling, the area of the ovipositor bearing the pheromone gland is extruded and exposed to the outside. Presence of extensive convolutions and cuticular hairs increases the surface area to facilitate the evaporation of the pheromone. When the pheromone is dissipated, the ovipositor is retracted thereby ‘squeezing’ more pheromone onto the exposed surface, followed by another extension. This sequence is repeated throughout the period of calling.

The pheromone gland in most species of moths had been referred to either as a single layer of columnar cells located in the ventral region, as distinct areas in both ventral and dorsal regions or as a continuos ring. Variations seen in the lepidopteran families were described by Percy-Cunningham and MacDonald (1987). In *H. zea*, the pheromone gland was found in the intersegmental membrane between the 8th and 9th abdominal segments (Jefferson et al., 1971; Aubrey et al., 1983; Percy-Cunningham and MacDonald, 1987). The structure was also erroneously referred to as a ring gland. Based on male activation assays, Srinivasan et al. (1986), reported that 81% of the activity in the navel orange worm, was present in the intersegmental region of the 8th and 9th segments. In the diamondback moth, Chow et al. (1976) suggested that the main sex pheromone gland was present in the 9th segment. Itagaki and Conner (1988) used dorsal and ventral portions of the pheromone gland bearing segments in *Manduca sexta* in conjunction with electroantennogram bioassays to show that maximal activity resided in the ventral portion. However, the activity was not significantly different from that in the dorsal portion. In *H. zea*, we corroborated for the first time histological evidence with chemical analysis to show that the pheromone gland occupied a nearly complete ring. In the retracted state of the ovipositor, the entire glandular area formed a U-shaped fold, thus preventing the release of pheromone by evaporation.

Most studies on the ultrastructure of pheromone glands in Lepidoptera described only one type of glandular cell. Hallberg and Subchev (1997) reported two cell types in the moth *Theresimima ampelophaga*, namely gland cells and wrapping cells. In *H. zea,* we also observed two distinct shapes of glandular cells that shared common features; the apical microvilli and pockets of granular material. Microvilli containing a core of smooth endoplasmic reticulum have been reported in *C. fumiferana* (Percy, 1974), and *T. ni* (Percy, 1979). Contrary to earlier reports, we did not observe Golgi bodies. Extensive basal invaginations were also reported in pheromone gland cells of *T. ampelophaga* (Hallberg and Subchev, 1997). Lipid spheres of varying sizes have been reported in the cytoplasm of pheromone gland cells in *C. fumiferana* (Percy, 1974), and *Argyrotaenia velutinana* (Feng and Roelofs, 1977). However, in *M. sexta*, Itagaki and Conner (1988) did not observe lipid droplets in the pheromone gland cells. In *T. ni*, pheromone glands produced pheromone soon after adult eclosion and production was continuous thereafter (Tang et al., 1991). Percy (1979) observed a major change in the size and abundance of lipid spheres between pre- and post-eclosion in *T. ni* glands. Recently, Zhao and Haynes (1997)

Fig. 5. (a, b and c). TEM micrographs of vertical sections through cuticular hairs or projections: (a) pore canals (arrows) in the epicuticle and the layered endocuticle; (b) electron dense material in the core of one of the projection and pore canals (arrows) in the epicuticle; (c) microvilli with pockets of granular material extended into the core of another projection; (d) LTSEM micrograph of cuticular hairs in the gland area showing droplets of excretion (arrows).

reported that in *T. ni*, transport of the pheromone to the gland surface is cyclic and possibly regulated by a PBAN like hormone. No such changes in the number and size of lipid droplets between photo- and scotophase were observed in *H. zea*. Recently, Fonagy et al. (2000) using the enzyme papain, separated the cellular layer from the cuticle in the pheromone gland area of *Bombyx mori* and demonstrated that only the former could produce the pheromone in vitro. They also reported that the synthesis could be stimulated by PBAN.

Since the above papers were published, a better understanding of pheromone biosynthesis in insects has been achieved (Tillman et al., 1999). In *H. zea*, the fatty acid precursor undergoes desaturation followed by reduction and oxidation to yield the major pheromone component (Jurenka et al., 1991). The final oxidation step is mediated by the enzyme alcohol oxidase present in the cuticle (Teal and Tumlinson, 1988). Therefore, the pheromone gland cells, besides producing the precursor, would be required to produce the necessary enzymes. Pheromone biosynthesis is activated during scotophase by PBAN. The material visualized in the intercellular canals and the pockets of granular material that we observed may represent various stages of the pheromone that was being synthesized.

In contrast to the knowledge about the structure of the pheromone glands in Lepidoptera, very little is known about the physical aspects of pheromone release. No well marked cuticular ducts have been seen leading from the pheromone gland as described in the cockroach (Liang and Schal, 1993). The presence of fine pores in the cuticle, including the cuticular hairs above the gland cells, and visualization of droplets of material, preserved by low temperature SEM technique may be indicative of the release of pheromone. Similar droplets have been reported in *M. sexta* (Itagaki and Conner, 1988). Interestingly, these droplets were only observed in the area of the pheromone gland and only in the scotophase females. These observations strengthen the assumption that the secretion may in fact be the pheromone. The pheromone gland occupies a rather narrow band, and to maximize the evaporation of the pheromone, it is smeared over a highly convoluted surface, during the rhythmic protrusion of the ovipositor, often referred to as calling.

Acknowledgements

We thank John Davis for his help in histology of the pheromone gland, G. C. Unnithan and P. E. A. Teal for critically reviewing the manuscript.

References

Aubrey, J.G., Boudreaux, H.B., Grodner, M.L., Hammond, A.M., 1983. Sex pheromone-producing cells and their associated cuticle in female *Heliothis zea* and *H. virescens* (Lepidoptera: Noctuidae). Annals of the Entomological Society of America 76, 343–348.

Chow, Y-S., Chen, J., Lin-Chow, S., 1976. Anatomy of female sex pheromone gland of the diamondback moth, *Plutella xylostella* (L.) (Lepidoptera: Plutellidae). International Journal of Insect Morphology and Embryology 5, 197–203.

Feng, K.C., Roelofs, W.L., 1977. Sex pheromone gland development in redbanded leafroller moth, *Argyrotaenia velutinana*, pupae and adults. Annals of the Entomological Society of America 70, 721–732.

Fonagy, A., Yokoyama, N., Okanu, K., Tatsuki, S., Maeda, S., Matsumoto, S., 2000. Pheromone-producing cells in the silkmoth, *Bombyx mori*: identification and their morphological changes in response to pheromonotropic stimuli. Journal of Insect Physiology 46, 735–744.

Hallberg, E., Subchev, M., 1997. Unusual location and structure of female pheromone glands in *Theresimima (= ino) ampelophaga* Bayle-Berelle (Lepidoptera: Zygaenidae). International Journal of Insect Morphology and Embryology 25, 381–389.

Itagaki, H., Conner, W.E., 1988. Calling behavior of *Manduca sexta* (L.) (Lepidoptera: Sphingidae) with notes on the morphology of the female sex pheromone gland. Annals of the Entomological Society of America 81, 798–807.

Jefferson, R.N., Shorey, H.H., Rubin, R.E., 1968. Sex pheromones of Noctuid moths. XVI. The female sex pheromone glands of eight species. Annals of the Entomological Society of America 61, 861–865.

Jefferson, R.N., Sower, L.L., Rubin, R.E., 1971. The female sex pheromone gland of the pink bollworm, *Pectinophora gossypiella* (Lepidoptera: Gelechiidae). Annals of the Entomological Society of America 64, 311–312.

Jurenka, R.A., Jacquin, E., Roelofs, W.L., 1991. Control of the pheromone biosynthetic pathway in *Helicoverpa zea* by the pheromone biosynthesis activating neuropeptide. Archives of Insect Biochemistry and Physiology 17, 81–91.

Klun, J.A., Plimmer, J.R., Bierl-Leonhardt, B.A., Sparks, A.N., Chapman, O.L., 1979. Trace chemicals: The essence of sexual communication systems in *Heliothis* species. Science 209, 1328–1330.

Liang, D., Schal, C., 1993. Ultrastructure and maturation of a sex pheromone gland in the female German cockroach, *Blattella germanica*. Tissue and Cell 25, 763–776.

Percy, J.E., 1974. Ultrastructure of pheromone gland cells and cuticle before and during release of pheromone in female eastern spruce budworm, *Choristoneura fumiferana* (Clem.) (Lepidoptera: Tortricidae). Canadian Journal of Zoology 52, 695–705.

Percy, J., 1979. Development and ultrastructure of sex-pheromone gland cells in females of the cabbage looper moth, *Trichoplusia ni* (Hubner) (Lepidoptera: Noctuidae). Canadian Journal of Zoology 57, 220–236.

Percy-Cunningham, J.E., MacDonald, J.A., 1987. Biology and ultrastructure of sex pheromone-producing glands. In: Prestwich, G.D., Blomquist, G.J. (Eds.). Pheromone Biochemistry. Academic Press, Orlando, FL, pp. 27–75.

Raina, A.K., Klun, J.A., Stadelbacher, E.A., 1986. Diel periodicity and effect of age and mating on female sex pheromone titer in *Heliothis zea* (Lepidoptera: Noctuidae). Annals of the Entomological Society of America 79, 128–131.

Raina, A.K., Jaffe, H., Kempe, T.G., Keim, P., Blacher, R.W., Fales, H.M., Riley, C.T., Klun, J.A., Ridgway, R.L., Hayes, D.K., 1989. Identification of a neuropeptide hormone that regulates sex pheromone production in female moths. Science 244, 796–798.

Spurr, A.R., 1969. A low viscosity epoxy resin embedding medium for electron microscopy. Journal of Ultrastructural Research 26, 31–43.

Srinivasan, A., Coffelt, J.A., Norman, P., Williams, B., 1986. Sex pheromone gland of the navel orangeworm, *Amyelois transitella* (Lepidoptera: Pyralidae) location, bioassay and in vitro maintenance. The Florida Entomologist 69, 169–174.

Tang, J.D., Wolf, W.A., Roelofs, W.L., Knipple, D.C., 1991. Development of functionally competent cabbage looper moth sex pheromone glands. Insect Biochemistry 21, 573–581.

Teal, P.E.A., Carlysle, T.C., Tumlinson, J.H., 1983. Epidermal glands in terminal abdominal segments of female *Heliothis virescens* (F.)

(Lepidoptera: Noctuidae). Annals of the Entomological Society of America 76, 242–247.

Teal, P.E.A., Tumlinson, J.H., 1988. Properties of cuticular oxidases used for sex pheromone biosynthesis by *Heliothis zea*. Journal of Chemical Ecology 14, 2131–2145.

Tillman, J.A., Seybold, S.J., Jurenka, R.A., Blomquist, G.J., 1999. Insect pheromones—an overview of biosynthesis and endocrine regulation. Insect Biochemistry and Molecular Biology 29, 481–514.

Wergin, W.P., Endo, B.Y., 1976. Ultrastructure of a neurosecretory organ in a root-knot nematode. Journal of Ultrastructural Research 56, 258–276.

Zhao, J.Z., Haynes, K.F., 1997. Does PBAN play an alternative role of controlling pheromone emission in the cabbage looper moth, *Trichoplusia ni* (Hubner) (Lepidoptera: Noctuidae)? Journal of Insect Physiology 43, 695–700.